



International Journal of Engineering and Technology Volume 3 No. 8, August, 2013

Design and Analysis of Ultra-Compact Plasmonic Sensor based on Waveguide-Coupled Structure

Jian Ping Guo^{1,2}, Jia Hu Zhu¹, Wen Zhou¹

¹Laboratory of Nanophotonic Functional Materials and Devices, South China Normal University, Guangzhou, 510006, China

²School of Physics and Telecommunication Engineering, South China Normal University, Guangzhou, 510006, China

ABSTRACT

Plasmonic waveguides-based sensors have many advantages in developing the compact on-chip surface plasmon resonance sensing systems. In this paper, a plasmonic refractive index sensor based on two waveguide-coupled cavities structure is proposed and demonstrated. The cavities are symmetrically located on two sides of the waveguide and could act as containers for the material under sensing. The finite difference time domain method is employed to study its sensing characteristics. The simulated results show that the resonant wavelengths of the sensor have a linear relationship with the refractive index of materials under sensing. Based on the relationship, the refractive index of the material can be obtained by detecting the resonant wavelength. Compared with the sensor with a single cavity, the sensor with two cavities has a similar response while has a larger transmission intensity due to the coupling effect between the cavities.

Keywords: *sensor; metal-insulator-metal ;waveguide; integrated optics devices*

I. INTRODUCTION

Since the first surface plasmon resonance (SPR) integrated optical sensors described in late 1980s [1], various integrated optical SPR sensors using slab waveguide, channel waveguide and even more complex waveguide structure have been demonstrated [2-6], but for most of conventional waveguides based sensors the diffraction limit of light poses a significant challenge to the miniaturization and ultra-density integration of optical circuits [7]. Plasmonic waveguides, based on surface plasmons polaritons (SPPs) propagating at the metal-dielectric interfaces, have been considered as one of promising candidates to overcome the classical diffraction limit for their ability to guide and manipulate light at deep subwavelength scales [7, 8]. A number of plasmonic waveguide structures have been proposed during the past decade [9]. Among those, waveguides consisted of an insulator sandwiched between two metals, serving as metal-dielectric-metal (MDM) waveguides or metal-insulator-metal (MIM) waveguides, can support propagating surface plasmon modes that are strongly confined in the insulator region with an acceptable propagation length [10,

11]. Their fabrication involves simple and cost-effective processes that are compatible with standard CMOS process for interchip interconnects. Therefore, MIM waveguides are promising for the design of nanoscale devices with a relatively easy fabrication according to the current state of the art. Compared with other type of sensors, plasmonic MIM waveguides integrated sensor has an inherent advantage to achieve high integration [8, 12].

Recently several plasmonic sensors have been investigated. Lu et al. [13] designed a nanosensor based on Fano resonance in the double nanoresonators system. Wu [14] and Chen [15] presented the experimental demonstration for a refractive index sensor based on the interference of two SPPs waves in the slit metallic structure. In this letter, a simple and compact plasmonic sensor based on symmetric metal-insulator-metal waveguide-coupled cavities structure is proposed. The physical mechanism of the device is deduced. The finite difference time domain (FDTD) method with a perfectly matched layer (PML) absorbing boundary condition is employed to simulate and study its properties.

II. DEVICE STRUCTURE AND THEORETICAL ANALYSIS

Fig. 1 shows the two-dimensional schematic map of the proposed sensor structure. It is consisted of a sub-wavelength MIM waveguide side-coupled to two cavities, which are filled with the material under sensing (MUS). The cavities are placed symmetrically on two sides of the waveguide while the waveguide is divided into two segments acting as input port and output port separated by a metal barrier, where w and w' stand for the width of the waveguide and cavities, L and L_{bar} are the lengths of the cavities and the barrier, respectively. w_{gap} denotes the gap distance between the waveguide and the MUS cavities. The metal here is assumed to be silver, whose frequency-dependent complex relative permittivity is characterized by the Drude model[16], and the dielectric in the waveguide is assumed to be SiO_2 with a refractive index $n=1.47$. The MUS cavities can be filled up with gaseous or liquid MUS with different methods. Simply gaseous MUS will be diffused into the cavities based on gas diffusion force in vacuum circumstance. Liquid MUS can be filled up into the cavities using nano-filling technique based on capillarity attraction[17]. First, part of the inner surface of the cavities are wetted by the liquid MUS. Secondly, the liquid penetrates into the cavities by the capillarity pumping effect, which makes the cavities full of the liquid MUS.

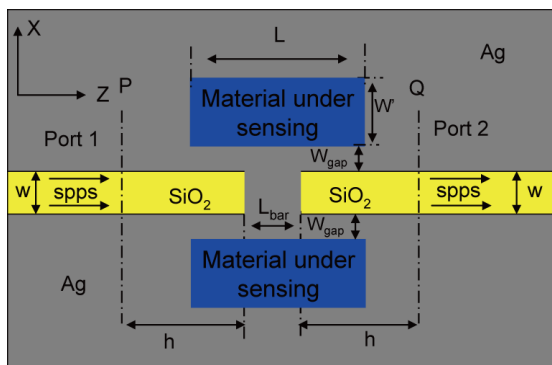


Fig. 1. a basic two-dimensional schematic map of the plasmonic refractive index sensor structure

The width of the waveguide is much smaller than the wavelengths of incident waves so that only the fundamental SPPs mode can be supported[11]. When a transverse magnetic(TM) mode is excited in the input port, part of the waves will be reflected at the front surface of metal barrier while the other part of the waves could be coupled into the upper and nether cavities due to the small width of the gap. The forward and backward waves in the cavities are almost completely reflected in the silver-air interfaces at both ends

until a standing waves is formed and then would be coupled forward into output port. Therefore, the structure operates like a Fabry–Perot resonance cavity. The resonance condition for a structure with a single cavity has been given by Mei[18]:

$$\lambda_m = \frac{2n_{eff}L}{m - \psi_r / \pi} \quad (m = 1, 2, 3, \dots), \quad (1)$$

where L is the length of the cavity, ψ_r is the phase shift of the beam reflected at one end of the cavity, n_{eff} is the real part of the effective index in the MUS cavity, whose value can be obtained by solving the dispersion relation of the fundamental TM mode in an MIM waveguide[16]:

$$\tanh\left(-\frac{ik_{z1}}{2}w'\right) = -\frac{\epsilon_m k_{z2}}{\epsilon_{MUS} k_{z1}}, \quad (2)$$

With k_{z1} and k_{z2} defined by momentum conservations:

$$\begin{cases} k_{z1}^2 = \epsilon_{MUS} k_0^2 - \beta^2 \\ k_{z2}^2 = \epsilon_m k_0^2 - \beta^2 \end{cases}, \quad (3)$$

here $\beta = \beta_R + i\beta_I$ is the complex propagation constant, $\epsilon_{MUS} = n_{MUS}^2$ and ϵ_m are the dielectric constants of the MUS and metal respectively. $k_0 = 2\pi / \lambda$ is the wave number of light in vacuum, w' is the width of the MUS cavity. The real part of the effective index in the MUS cavity n_{eff} is given by $n_{eff} = \beta_R / k_0$ [19]. The relationship between n_{eff} and n_{MUS} is calculated and shown in Fig.2. It can be seen that the n_{eff} is linear to the n_{MUS} at all wavelengths. Based on the relationship the sensor can be operated as followed: Firstly the MUS cavities are filled up with different materials whose refractive indices are known and the resonant wavelength of the transmission spectrum is detected respectively, the calibration curve of the sensor can be obtained as the resonant wavelength versus the refractive index. And then an unknown MUS is put into the cavities and the transmission spectrum is detected, one can get its refractive index by using the calibration curve. Thus a plasmonic sensor device will be achieved.

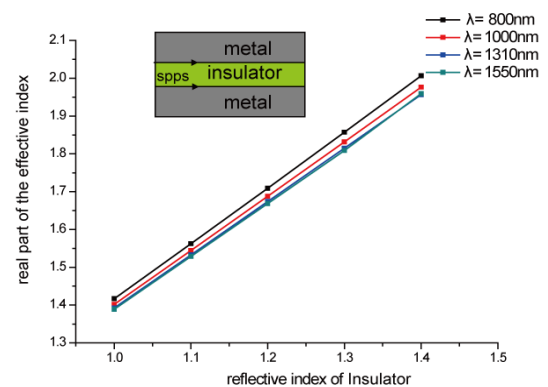


Fig. 2.

The real part of the effective index n_{eff} versus the refractive index n of the insulator in an MIM waveguide structure ($w'=50\text{nm}$) for different incident wavelengths $\lambda = 800, 1000, 1310, \text{ and } 1550\text{nm}$.

III. SIMULATION RESULTS AND DISCUSSION

In order to investigate the characteristics of the plasmonic sensor, the FDTD method is employed to calculate the transmission spectra of the proposed structure. In the following FDTD simulations, the grid sizes in both the x and the z directions are chosen to be 2.5 nm . PML absorbing boundary condition is used at all boundaries of the simulation domain. Power monitors are set at the positions of P and Q to detect the incident power of P_{in} and the transmitted power of P_{out} . The transmittance is defined to be $T=P_{out}/P_{in}$. During the simulation, the width of the waveguide w and the lengths of the the barrier L_{bar} is fixed to be 50 nm and 100nm respectively while other parameters are changeable.

At first, we can assume that the two MUS cavities are filled with air, whose refractive index is equal to 1. For the structure with the parameters of $L=300\text{ nm}$, $h=150\text{ nm}$, $w'=50\text{ nm}$, and $W_{gap}=20\text{ nm}$, the transmission spectrum of the structure is shown in Fig. 3. It can be seen that there is a resonant wavelength at 970.3nm with a maximum transmission about 71.4% .

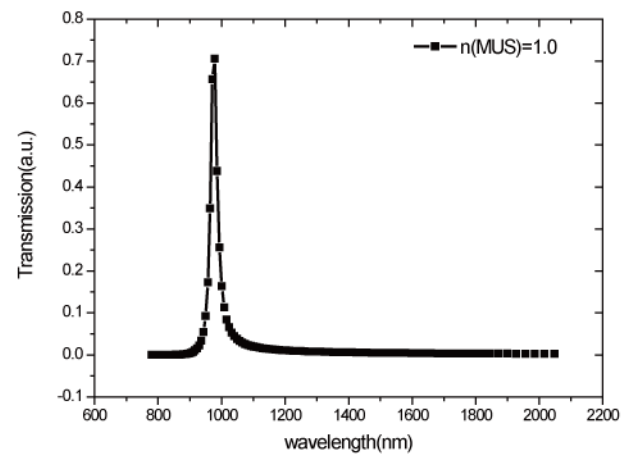


Fig. 3. Transmission spectra of the symmetrical side-coupled cavities sensor structure with $L=300\text{ nm}$, $L_{bar}=100\text{nm}$, $h=150\text{ nm}$, $w'=50\text{ nm}$, and $W_{gap}=20\text{ nm}$

Now the cavities would be in turn filled with different materials whose refractive indices have been known to us. Fig. 4(a) shows the simulated results of transmission spectra of the sensor structure for different refractive indices while the geometric parameters of sensor are kept as the same as those in the Fig. 3. The resonant wavelengths show a redshift as the refractive index n is increased. When the refractive index is increased from 1 to 1.60, the resonant wavelength shifts from 970.3nm to 1573.5nm . Fig. 4(b) displays the linear relationship between the resonant wavelengths and the refractive index. It can be seen that the shift of resonant wavelengths as the function of the refractive index is equal to $1005.3\text{ nm per refractive index unit (RIU)}$, which is moderate as compared with other SPR on-chip platforms[20].

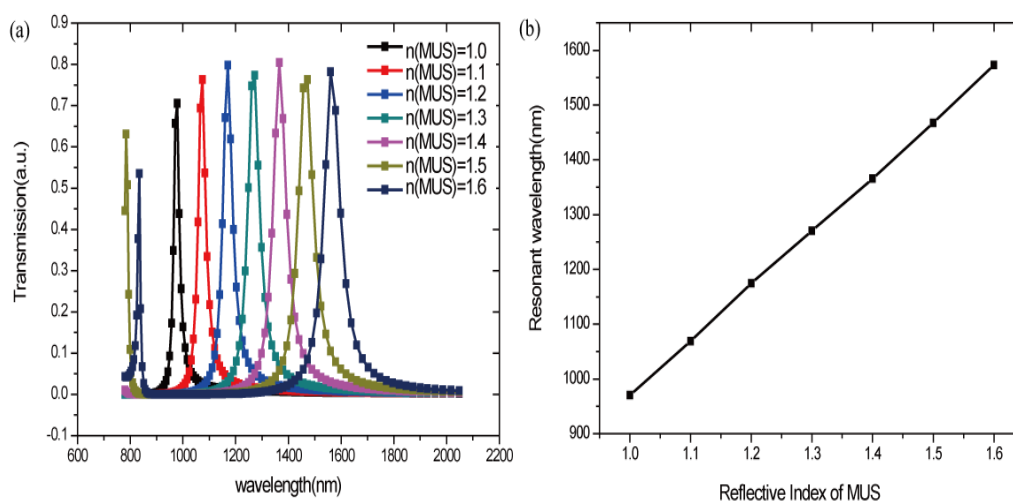


Fig. 4 (a) Simulated reflection spectra of the sensor in different refractive indices n_{MUS} with the slit $L = 300\text{ nm}$ and $w'=50\text{ nm}$; (b) the resonant wavelength of the transmission spectrum shown in (a) versus the refractive index n of the MUS.

When the MUS cavities are filled with a unknown material, if the resonant wavelength of the sensor is measured to be 1250nm, from the Fig. 4(b), the refractive index n_{MUS} is obtained to be 1.222.

In order to make a comparison, the transmission spectrum of the plasmonic sensor with a single cavity is also calculated. Fig. 5 shows the simulated results of transmission spectra of the sensor with a single cavity for different refractive indices. The geometric parameters of sensor are kept as the same as those in the Fig. 3 and Fig.4. The plasmonic sensor with a single cavity has a similar transmission spectrum with that of the sensor with two cavities, but at each resonant wavelength it has a smaller transmission intensity than the latter.

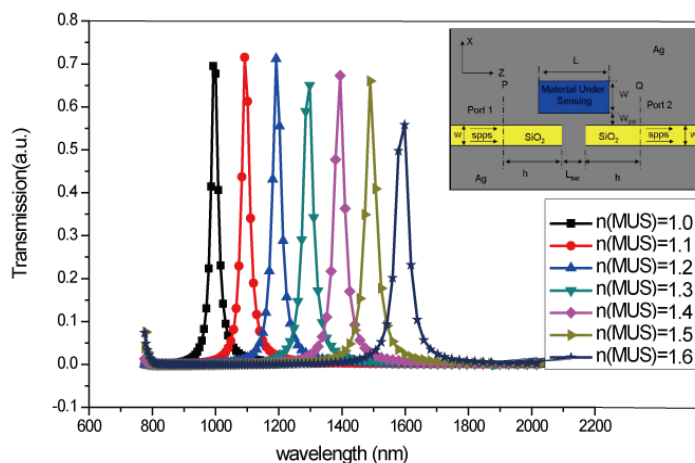


Fig. 5

Simulated reflection spectra of the sensor with a single cavity in different refractive indices n_{MUS} , Inset: schematic map of the plasmonic refractive index sensor with a single cavity

Fig. 6 show the comparison of the transmission spectrum versus the refractive index n of the MUS between the sensor with a single cavity and two cavities. It can be seen clearly from the figure that for the same refractive index n of the MUS, sensor with a single cavity has longer resonant wavelengths than those of the sensor with double cavities. Such phenomenon could be simply contributed to the coupling effect between the two cavities. For the sensor with two cavities, the waves in the upper and nether cavities couple to each other vs the waveguide between them, which means the width of the both cavities could be broaden in a sense. From the Eqs. (1) and (2), a smaller resonant wavelength would be achieved as a result.

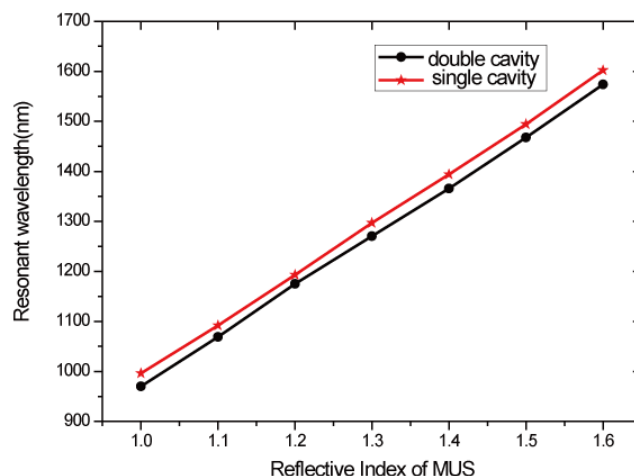


Fig. 6

Comparison of the resonant wavelength of the transmission spectrum versus the refractive index n of the MUS between the sensor with different cavities

IV. CONCLUSION

In conclusion, a plasmonic refractive index sensor based on waveguide-coupled cavities structure is introduced and demonstrated. The resonant wavelengths of the sensor have a linear relationship with the refractive index of materials under sensing. The sensor with two cavities has a similar response curve as the sensor with single cavity while has a larger transmission intensity. The structure has a compact size with hundreds of nanometer in width and length. Thus the device would be an important step toward a fully integrated surface plasmon lab-on-chip solution, which means that it may be used in high-resolution chemical and biological detections.

Acknowledgements

The authors thank Professor Xuguang Huang for helpful discussions. This work was supported by the National Natural Science Foundation of China(No.61275059), Excellent Young Teachers Program of SCNU (No.2012KJ002) and “973” Project (No.2011CBA00200).

REFERENCES

[1]. H. J. M. Kreuwel, P. V. Lambeck, J. v. Gent, and T. J. A. Popma, Surfaceplasmon dispersion and luminescence quenching applied to a planar waveguide sensors for

- measurement of chemical concentrations, Proc. SPIE **789** (1987) 218-224.
- [2]. C. R. Lavers, and J. S. Wilkinson, A waveguide-coupled surface plasmon resonance sensor for an aqueous environment, Sensors and Actuators B: Chemical **22**, (1994) 475-481.
- [3]. R. D. Harris, and J. S. Wilkinson, Waveguide surface plasmon resonance sensors, Sensors and Actuators B: Chemical **29** (1995) 261-267.
- [4]. R. Levy, A. Peled, and S. Ruschin, Waveguided SPR sensor using a Mach-Zehnder interferometer with variable power splitting ratio, Sensors and Actuators B: Chemical **119**, (2006) 20-26.
- [5]. J. R. Krenn, N. Galler, H. Ditlbacher, A. Hohenau, B. Lamprecht, E. Kraker, G. Jakopic, and T. Mayr, Waveguide-integrated SPR sensing on an all-organic platform Proc. SPIE **8073**, (2011) 80730F.
- [6]. Y. Yuan, L. Ding, and Z. Guo, Numerical investigation for SPR-based optical fiber sensor, Sensors and Actuators B: Chemical **157**, (2011) 240–245.
- [7]. W. Barnes, A. Dereus, and T. Ebbesen, Surface plasmon subwavelength optics, Nature **424**, (2003) 824-830.
- [8]. D. Gramotnev, and S. Bozhevolnyi, Plasmonics beyond the diffraction limit, Nature Photonics **4**, (2010) 83-91.
- [9]. S. I. Bozhevolnyi, *Plasmonic Nanoguides and Circuits* (Pan Stanford Publishing Pte. Ltd., Singapore, 2009).
- [10]. G. Veronis, Z. Yu, S. Kocabas, D. Miller, M. Brongersma, and S. Fan, Metal-dielectric-metal plasmonic waveguide devices for manipulating light at the nanoscale, Chinese Optics Letters **7**:(2009) 302-308.
- [11]. J. Dionne, L. Sweatlock, H. Atwater, and A. Polman, Plasmon slot waveguides: Towards chip-scale propagation with subwavelength-scale localization, Physical Review B **73**, (2006)
- [12]. E. Ozbay, Plasmonics: Merging Photonics and Electronics at Nanoscale Dimensions, Science **311**, (2006) 189-193.
- [13]. H. Lu, X. Liu, D. Mao, and G. Wang, Plasmonic nanosensor based on Fano resonance in waveguide-coupled resonators, Optics Letters **37**, (2012) 3780-3782.
- [14]. X. Wu, J. Zhang, J. Chen, C. Zhao, and Q. Gong, Refractive index sensor based on surface-plasmon interference, Optics Letters **34**, (2009)
- [15]. W. Chen, C. Jian-Jun, T. Wei-Hua, and X. Jing-Hua, Ultracompact Refractive Index Sensor Based on Surface-Plasmon-Polariton Interference, Chinese Physics Letters **29**, (2012) 127304.
- [16]. Z. Han, E. Forsberg, and S. He, Surface plasmon Bragg gratings formed in metal-insulator-metal waveguides, IEEE Photonics Technology Letters **19**, (2007) 91-93.
- [17]. A. Y. Vorobyev, and C. Guo, Metal pumps liquid uphill, Applied Physics Letters **94**, (2009) 224102.
- [18]. X. Mei, X. Huang, J. Tao, J. Zhu, Y. Zhu, and X. Jin, A wavelength demultiplexing structure based on plasmonic MDM side-coupled cavities, Journal of the Optical Society of America B- Optical Physics **27**, (2010) 2707-2713.
- [19]. X.-S. Lin, and X.-G. Huang, Tooth-shaped plasmonic waveguide filters with nanometeric sizes, Optics Letters **33**, (2008) 2874-2876.
- [20]. D.-J. Lee, H.-D. Yim, S.-G. Lee, and B.-H. O, Tiny surface plasmon resonance sensor integrated on silicon waveguide based on vertical coupling into finite metal-insulator-metal plasmonic waveguide, Optics Express **19**, (2011) 19895-19900.